J|A|C|S
ARTICLES

Published on Web 03/17/2009

Hydration of Protonated Aromatic Amino Acids: Phenylalanine, Tryptophan, and Tyrosine

Bing Gao, Thomas Wyttenbach, and Michael T. Bowers*

Department of Chemistry and Biochemistry, University of California, Santa Barbara, California 93106-9510

Received October 29, 2008; E-mail: bowers@chem.ucsb.edu

Abstract: The first steps of hydration of the protonated aromatic amino acids phenylalanine, tryptophan, and tyrosine were studied experimentally employing a mass spectrometer equipped with a drift cell to examine the sequential addition of individual water molecules in equilibrium experiments and theoretically by a combination of molecular mechanics and electronic structure calculations (B3LYP/6-311++G**) on the three amino acid systems including up to five water molecules. It is found that both the ammonium and carboxyl groups offer good water binding sites with binding energies of the order of 13 kcal/mol for the first water molecule. Subsequent water molecules bind less strongly, in the range of 7−11 kcal/mol for the second through fifth water molecules. The ammonium group is able to host up to three water molecules and the carboxyl group one water molecule before additional water molecules bind either to the amino acid side chain as in tyrosine or to already-bound water in a second solvation shell around the ammonium group. Reasons for the surprisingly high water affinity of the neutral carboxyl group, comparable to that of the charge-carrying ammonium group, are found to be high intrinsic hydrophilicity, favorable charge−dipole alignment, and − for the case of multiply hydrated species − favorable dipole−dipole interaction among water molecules and the lack of alternative fully exposed hydration sites.

Introduction

In living cells, normal function requires that proteins participate in very specific reactions, which can take place only if the proteins possess the correct conformations. As a physical process, protein folding to the correct conformation in solution requires a specific set of circumstances such that the desired state is favored thermodynamically and is soluble.[1] Water is such a solvent where these two criteria can be satisfied and therefore plays an important and unique role in the protein folding pathway.[2] As a protein folds, many of the hydrogen bonds between water and the individual amino acids that make up the protein chain break, and new hydrogen bonds form in the various intermediates that lead to the native state of the protein along the folding pathway.[3−6] Thus, in recent decades, the interaction of proteins with surrounding water has become an intriguing subject to scientists.[7,8]

Of the numerous experimental methods available for these types of investigations, mass spectrometry provides an ideal technique to examine biomolecule hydration on a molecular level by studying sequential addition of individual water molecules. This has been recently made possible with the development of soft ionization techniques that allow fragile biomolecules to be transferred from solution into the gas phase without fragmentation.[9] Mass spectrometry allows us to systematically investigate the most basic biomolecule−water interactions in a controlled manner and also sheds light on the relationship between biomolecule structures in the solvent and gas phases and the role that water plays in structure.

In our group, ion mobility mass spectrometry was used to study structure and early aggregation of the Aβ protein, whose pathological folding and aggregation are responsible for onset and development of Alzheimer's disease.[10,11] The experimental results together with theoretical calculations have shown that, in the hydrated Aβ42 structure, the hydrophobic portions of the protein strongly interact in the interior of the structure while the hydrophilic segments are found on the exterior, interacting with H_2O molecules. In contrast, the solvent-free conformation is much more compact, with the hydrophobic components exposed at the surface. The hydrophilic groups cluster inside, benefiting from self-solvation. This example shows the important role water plays in protein conformation. It is clear that, to fully understand the mechanism of peptide and protein folding and

(1) Pace, C. N.; Trevino, S.; Prabhakaran, E.; Scholtz, J. M. *Philos. Trans. R. Soc. B* **2004**, *359*, 1225–1234.
(2) Mattos, C.; Clark, A. C. *Arch. Biochem. Biophys.* **2008**, *469*, 118–131.
(3) Shortle, D. *Nat. Struct. Biol.* **1999**, *6*, 203–205.
(4) Cheung, M. S.; Garcia, A. E.; Onuchic, J. N. *Proc. Natl. Acad. Sci. U.S.A.* **2002**, *99*, 685–690.
(5) Brun, L.; Isom, D. G.; Velu, P.; Garcia-Moreno, B.; Royer, C. A. *Biochemistry* **2006**, *45*, 3473–3480.
(6) Papoian, G. A.; Ulander, J.; Eastwood, M. P.; Luthey-Schulten, Z.; Wolynes, P. G. *Proc. Natl. Acad. Sci. U.S.A.* **2004**, *101*, 3352–3357.
(7) Ball, P. *Chem. Rev.* **2008**, *108*, 74–108.
(8) Fullerton, G. D.; Cameron, I. L. *Methods Enzymol.* **2007**, *428*, 1–ff.
(9) Wyttenbach, T.; Bowers, M. T. *Annu. Rev. Phys. Chem.* **2007**, *58*, 511–533.
(10) Baumketner, A.; Bernstein, S. L.; Wyttenbach, T.; Bitan, G.; Teplow, D. B.; Bowers, M. T.; Shea, J. E. *Protein Sci.* **2006**, *15*, 420–428.
(11) Bernstein, S. L.; Wyttenbach, T.; Baumketner, A.; Shea, J. E.; Bitan, G.; Teplow, D. B.; Bowers, M. T. *J. Am. Chem. Soc.* **2005**, *127*, 2075–2084.

its dependence on amino acid sequence, it is essential to explore the interactions between amino acids and their surrounding H_2O molecules.

In addition to the ion mobility experiments, our group initiated several studies on the interactions between small peptides and water using a high-pressure drift cell for temperature-dependent equilibrium experiments.[12−15] These experiments give us thermodynamic values for hydration as well as information about the extent of solvation and solvation shell size. Our investigations have shown that hydration of small peptides is largely controlled by its charged groups. For instance, the extent of solvation correlates with the number of charges: peptides with more charges bind more water molecules.[12] Experiment and theoretical modeling have shown that a peptide's charged groups (the ammonium, guanidinium, and carboxylate groups) normally serve as hydration sites, with binding energies on the order of 10 kcal/mol, with corresponding hydration entropy changes of about 20 cal/(mol·K). Variations in these values as a function of charged group identity and the influence of competition between multiple charged groups have been explored.[15] Competition between self-solvation and hydration, as well as conformation change upon hydration, has also been investigated.[14]

Hydration of a number of amino acids was also studied in other groups employing equilibrium[16−20] and other techniques including theory. A recent high-pressure mass spectrometry study provided thermodynamic information for a range of protonated amino acids (including Phe, but not Tyr and Trp) with up to four water molecules.[16,17] However, the study did not include a detailed analysis of hydration sites. Theoretical studies, on the other hand, give detailed structural information and are often a useful supplement to experiment. For instance, a calculation for $GlyH^+ \cdot H_2O$ on a high level of theory[21] showed that water binds preferentially to the ammonium group, although a number of alternative hydration sites, including the carboxyl group, were identified as well. Similar conclusions were obtained in a theoretical investigation on $AlaH^+ \cdot H_2O$ carried out in an attempt to understand the gas-phase H/D exchange mechanism occurring in this system.[22] Theoretical work combined with careful blackbody infrared radiative dissociation studies yielded information about water binding energies and binding sites on cationized amino acids,[23,24] and thorough spectroscopic studies on several protonated amino acids, including Val, Tyr, and Trp, provided detailed structural information of the hydrated species with up to four water molecules.[25−27]

In these spectroscopic studies, Rizzo and co-workers have probed vibrational and electronic transitions to investigate microsolvation. Infrared spectra clearly show that the charged ammonium is the primary hydration site for $ValH^+ \cdot (H_2O)_n$ ($n = 1-4$) and competition for water by the carboxyl group increases with the water cluster size.[25] For gaseous protonated tryptophan, the ultracold (~10 K) electronic spectra show that the addition of H_2O molecules lengthens the excited-state lifetime, which indicates that the hydration of $TrpH^+$ has an impact on the dynamics of photoexcitation.[26,27] These outstanding spectroscopic studies shed light on the details of biomolecule−water interaction at the molecular level.

In this study, we employ hydration equilibrium measurements together with theoretical calculations to investigate the interaction of the protonated aromatic amino acids phenylanaline, tryptophan, and tyrosine with H_2O molecules focusing on water binding energies, water binding sites, and other structural aspects.

Methods

Hydration Equilibrium Measurement. The instrumentation used here has previously been described in detail.[12,28] Briefly, ions produced by electrospray ionization (ESI), entering the vacuum system through a metal capillary, are subsequently guided by an ion funnel through two stages of differential pumping and are finally injected into a drift cell filled with 0.1−1.4 Torr water vapor. The cell pressure is limited at higher temperature by the instrument pumping capacity and at cold temperature by the water pressure over ice. The temperature of the cell is adjustable, with cooling provided by a liquid nitrogen cooling system and heating by electrical heaters. The ions drift through the cell under the influence of a weak uniform electric field while undergoing many thousands to millions of collisions with water molecules, thereby establishing an equilibrium of hydrated ions. The hydrated ions leaving the drift cell are mass analyzed in the quadrupole mass filter following the drift cell and then detected.

All of the samples were purchased from Sigma and used without further purification. Samples were typically sprayed from a ~100 μM solution (water:methanol:acetic acid, 50%:50%:0.1%) using a metal-coated glass ESI spray tip in the electrospray arrangement.[28]

In the hydration experiment, the reaction shown in eq 1 is investigated.

$$MH^+ \cdot (H_2O)_{n-1} + H_2O \rightleftharpoons MH^+ \cdot (H_2O)_n \qquad (1)$$

The intensity I_n of the $MH^+ (H_2O)_n$ peak in the hydration equilibrium mass spectrum is proportional to the concentration of the $[MH^+ \cdot (H_2O)_n]$ species. Hence, the equilibrium constant K_n for eq 1 can be determined from the intensity ratio (I_n/I_{n-1}) and the known water pressure $P(H_2O)$ as shown in eq 2.

$$K_n = \frac{[MH^+ \cdot (H_2O)_n] \cdot 760\ \text{Torr}}{[MH^+ \cdot (H_2O)_{n-1}] \cdot P(H_2O)} = \frac{I_n}{I_{n-1}} \cdot \frac{760\ \text{Torr}}{P(H_2O)} \qquad (2)$$

(12) Liu, D. F.; Wyttenbach, T.; Barran, P. E.; Bowers, M. T. *J. Am. Chem. Soc.* **2003**, *125*, 8458–8464.
(13) Wyttenbach, T.; Paizs, B.; Barran, P.; Breci, L.; Liu, D. F.; Suhai, S.; Wysocki, V. H.; Bowers, M. T. *J. Am. Chem. Soc.* **2003**, *125*, 13768–13775.
(14) Liu, D. F.; Wyttenbach, T.; Carpenter, C. J.; Bowers, M. T. *J. Am. Chem. Soc.* **2004**, *126*, 3261–3270.
(15) Wyttenbach, T.; Liu, D. F.; Bowers, M. T. *Int. J. Mass Spectrom.* **2005**, *240*, 221–232.
(16) Wincel, H. *Int. J. Mass Spectrom.* **2006**, *251*, 23–31.
(17) Wincel, H. *Chem. Phys. Lett.* **2007**, *439*, 157–161.
(18) Meotner, M.; Field, F. H. *J. Am. Chem. Soc.* **1974**, *96*, 3168–3171.
(19) Blades, A. T.; Klassen, J. S.; Kebarle, P. *J. Am. Chem. Soc.* **1996**, *118*, 12437–12442.
(20) Kohtani, M.; Breaux, G. A.; Jarrold, M. F. *J. Am. Chem. Soc.* **2004**, *126*, 1206–1213.
(21) Michaux, C.; Wouters, J.; Jacquemin, D.; Perpete, E. A. *Chem. Phys. Lett.* **2007**, *445*, 57–61.
(22) Rozman, M. *J. Am. Soc. Mass Spectrom.* **2005**, *16*, 1846–1852.
(23) Lemoff, A. S.; Williams, E. R. *J. Am. Soc. Mass Spectrom.* **2004**, *15*, 1014–1024.
(24) Lemoff, A. S.; Bush, M. F.; Wu, C. C.; Williams, E. R. *J. Am. Chem. Soc.* **2005**, *127*, 10276–10286.
(25) Kamariotis, A.; Boyarkin, O. V.; Mercier, S. R.; Beck, R. D.; Bush, M. F.; Williams, E. R.; Rizzo, T. R. *J. Am. Chem. Soc.* **2006**, *128*, 905–916.
(26) Boyarkin, O. V.; Mercier, S. R.; Kamariotis, A.; Rizzo, T. R. *J. Am. Chem. Soc.* **2006**, *128*, 2816–2817.
(27) Mercier, S. R.; Boyarkin, O. V.; Kamariotis, A.; Guglielmi, M.; Tavernelli, I.; Cascella, M.; Rothlisberger, U.; Rizzo, T. R. *J. Am. Chem. Soc.* **2006**, *128*, 16938–16943.
(28) Wyttenbach, T.; Kemper, P. R.; Bowers, M. T. *Int. J. Mass Spectrom.* **2001**, *212*, 13–23.

The equilibrium constant is averaged over several measurements carried out at variable pressure at constant temperature and produces the free energy ΔG_n^0 (eq 3). Evaluating a plot of ΔG_n^0 versus temperature T (eq 4) yields values for the hydration enthalpies ΔH_n^0 (intercept) and the hydration entropies ΔS_n^0 (slope).

$$\Delta G_n^0 = -RT \ln K_n \tag{3}$$

$$\Delta G_n^0 = \Delta H_n^0 - T\Delta S_n^0 \tag{4}$$

Uncertainties in the ΔH_n^0 and ΔS_n^0 values reported here are based on the average statistical error (one standard deviation) obtained in least-squares fits to the ΔG_n^0 versus T data.

Theoretical Calculations. Some of the problems often encountered in calculations of hydrated polyatomic ions include the floppiness of the structures involved and the existence of many isomers with small energy differences, making it difficult to obtain all relevant structures by static quantum chemical methods. Employing molecular dynamic simulations is an effective tool to overcome these problems.[13,25,29,30] Here we employ molecular-mechanics (MM) dynamics simulations as implemented in Amber 8.[31] The starting structure for a dynamics calculation of a hydrated species is generally obtained by adding water molecules to the quantum-chemically optimized geometry of the dehydrated species using chemical intuition for the placement of water. After 30 ps of dynamics at 600 K, the heated hydrated ion is subjected to a cooling run of 10 ps to 50 K. The thermally annealed structure is minimized in the *ff03* force field.[31] By repeating the above simulated annealing procedure, 100 candidates are generated for further structure selection and optimization.

The 100 candidate structures are categorized into groups according to the site of hydration, such as ammonium, carboxyl, and side-chain functional groups. From each group containing often a large number of very similar structures, especially for multiply hydrated ions, the geometry with the lowest energy is chosen as a representative of the group and used as the starting point for a quantum chemical calculation. Using the Gaussian03 package,[32] the selected structures are optimized at the B3LYP/6-311++G** level. Vibrational frequencies are calculated to verify the nature of the stationary structure for all ions. The basis set superposition error (BSSE) is corrected by the counterpoise correction scheme[33,34] during the optimization. Final energy values reported here are, in addition, corrected for zero-point energy and, in the case of ΔH_n^0 values, for thermal (298 K) energy.

To independently examine the energy ordering obtained by B3LYP/6-311++G**, we performed full geometry optimizations of the $ValH^+ \cdot (H_2O)_2$ structures **C** and **D** (see Results) at the MP2 level using the 6-311++G** basis set. BSSE correction is carried out during the optimization.

Results

Experimental Hydration Equilibrium Data. Figure 1 shows two mass spectra of protonated tryptophan (Trp) hydrated at 399 and 242 K, respectively. Similar spectra are also obtained for phenylalanine (Phe) and tyrosine (Tyr). At 399 K and 1.2 Torr of water pressure, protonated Trp picks up a maximum of one H_2O molecule, whereas at 242 K, as many as five or six H_2O molecules stick to the ion, even at a pressure of only ~0.21 Torr. The ΔG_n^0 vs T plot, shown in Figure 2 for protonated Trp, indicates a linear relationship yielding the hydration enthalpy and entropy values listed in Table 1.

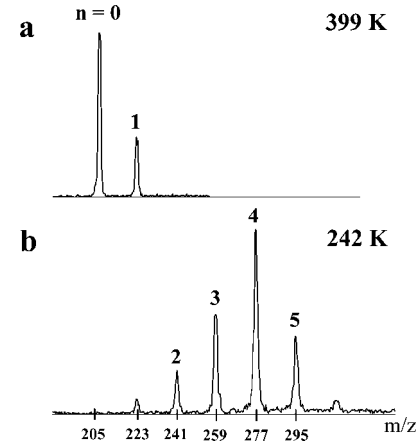

Figure 1. Mass spectra for the hydration of protonated tryptophan (n = number of water molecules) measured (a) at a temperature of 399 K with a pressure of ~1.2 Torr and (b) at a temperature of 242 K with a pressure of 0.21 Torr.

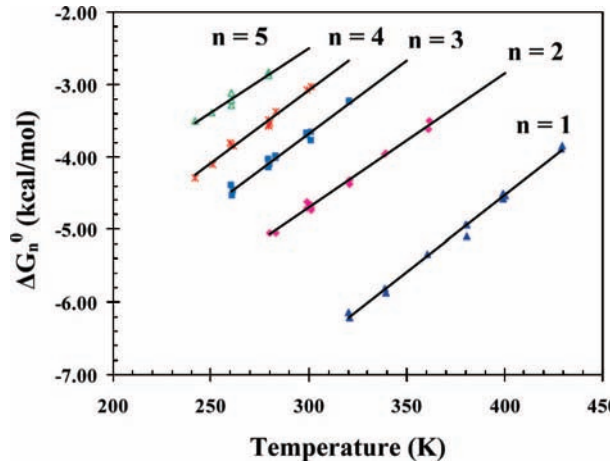

Figure 2. Plots of ΔG_n^0 vs T for the hydration of protonated Trp. Values of ΔH_n^0 (y-axis intercept) and ΔS_n^0 (slope) obtained from these plots are derived from the measured temperature-dependent equilibrium constants according to eqs 2−4.

The data in Figure 3 and Table 1 indicate a gradual decrease in the experimental water binding energy from 13 to 8 kcal/mol with increasing number n of H_2O molecules. The only exception to the steady decrease of $-\Delta H_n^0$ appears to be the step from $n = 4$ to 5 for Phe and Trp, which is larger than expected based on the trend established by the $n \leq 4$ data.

The sequential hydration entropies (ΔS_n^0) are −20 cal/(mol·K), more or less independent of n for nearly all values of n and all amino acids. However, while $-\Delta S_5$ for Tyr is comparable to $-\Delta S_1$ through $-\Delta S_4$, for Phe and Trp there is a clear drop from $-\Delta S_4$ to $-\Delta S_5$ by 28% and 20%, respectively.

Theoretical Structures. Typical lowest-energy representatives for a range of families of structures are shown in Figures 4 and 5, with structures grouped into families by similarity of hydration pattern (water binding sites). The structures in Figures 4 and 5 represent DFT-optimized geometries of protonated Phe, Trp, and Tyr in the presence of one or several H_2O molecules. Structures **A** and **B** are the two energetically most favorable geometries of the singly hydrated species. Hydration of the ammonium group (in **A**) and hydration of the carboxyl group

(29) Gao, B.; Liu, Z. F. *J. Chem. Phys.* **2005**, *123*, 224302.
(30) Bleiholder, C.; Osburn, S.; Williams, T. D.; Suhai, S.; Stipdonk, M. V.; Harrison, A. G.; Paizs, B. *J. Am. Chem. Soc.* **2008**, *130*, 17774–17789.
(31) Case, D. A.; et al. *Amber 8*; University of California, San Francisco, 2004.
(32) Frisch, M. J.; et al. *Gaussian 03*, Revision C.02; Gaussian Inc.: Wallingford, CT, 2004.
(33) Simon, S.; Duran, M.; Dannenberg, J. J. *J. Chem. Phys.* **1996**, *105*, 11024–11031.
(34) Boys, S. F.; Bernardi, F. *Mol. Phys.* **1970**, *19*, 553–&.

Table 1. Experimentally Measured ΔH_n^0 (kcal/mol) and ΔS_n^0 (cal/(mol·K)) and Calculated ΔH_n^0 (kcal/mol) Values for Protonated Phenylalanine, Tryptophan, and Tyrosine (289 K)

	Phe			Trp			Tyr		
n	$-\Delta H_n^{0a}$ (kcal/mol)	$-\Delta S_n^{0a}$ (cal/mol·K)	$-\Delta H_n^{0b}$ (kcal/mol)	$-\Delta H_n^{0a}$ (kcal/mol)	$-\Delta S_n^{0a}$ (cal/mol·K)	$-\Delta H_n^{0b}$ (kcal/mol)	$-\Delta H_n^{0a}$ (kcal/mol)	$-\Delta S_n^{0a}$ (cal/mol·K)	$-\Delta H_n^{0b}$ (kcal/mol)
1	13.3	20.2	14.6	13.2	21.7	13.8	13.6	21.6	14.4
2	11.3	19.9	11.9	10.7	19.8	12.6	10.6	18.0	12.5
3	10.3	20.9	9.8	9.7	20.3	10.1	9.2	17.1	10.7
4	9.7	21.6	9.4	9.1	20.3	9.6	9.4	20.9	8.9
5	7.4	15.4	8.3	7.5	16.6	8.4	8.6	20.5	8.1

[a] The experimentally measured values have uncertainties of ±0.5 kcal/mol for enthalpies and ±1.6 cal/(mol·K) for entropies (see Methods). [b] Uncertainty of calculated values is of the order of ±1 kcal/mol (see Discussion).

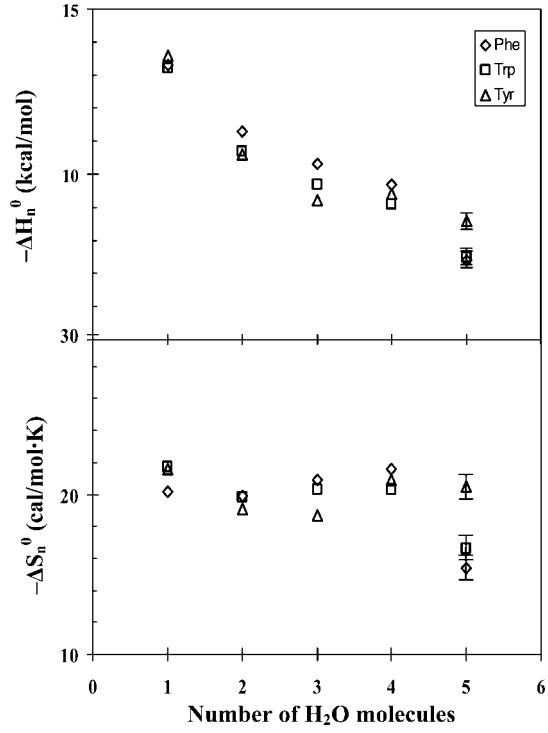

Figure 3. $-\Delta H_n^0$ vs n (upper plot) and $-\Delta S_n^0$ vs n (lower plot) for the hydration of protonated phenylalanine, tryptophan, and tyrosine (n = number of water molecules). Uncertainties are ±0.5 kcal/mol for enthalpies and ±1.6 cal/(mol·K) for entropies, as indicated by the bars for the example of $n = 5$.

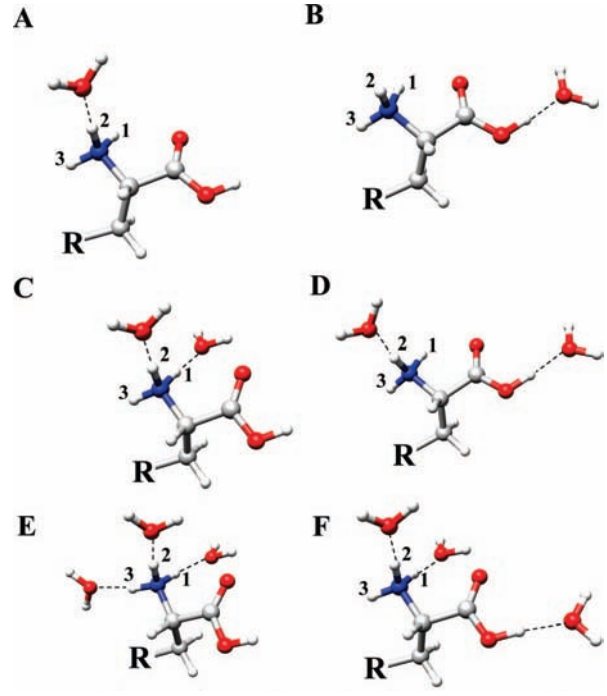

Figure 4. Hydration structures for protonated Phe, Trp, and Tyr with one (**A**,**B**), two (**C**,**D**), and three (**E**,**F**) H_2O molecules. At each particular size, two competitive hydration geometries are shown. R represents the side chain in each amino acid. (R = C_6H_5, C_8NH_6, and C_6H_4OH for Phe, Trp, and Tyr, respectively.) Coordinates for all structures given in Supporting Information.

(in **B**) are within 1 kcal/mol (Table 2) for all three amino acids Phe, Trp, and Tyr.

Structures **C** and **D** indicate that the second water molecule either adds to the ammonium group like the first water or adds to the carboxyl OH group. Both structures are nearly isoenergetic within the precision of the calculation, given that structure **D** (carboxyl group addition) is lower in energy by only 0.7−1.7 kcal/mol for Phe, Trp, and Tyr on the B3LYP level of theory.

Structures **E** and **F** are representatives of triply hydrated amino acids with similar energies, where the ammonium group is the primary site of hydration hosting either two (**F**) or three (**E**) H_2O molecules.

Structures **G**−**J** (Figure 5) are examples of more extensively hydrated species. In **G** all four hydration sites observed in **A**−**F** are occupied simultaneously. In **H** a fifth H_2O molecule binds to two previously added H_2O molecules, starting a second solvation shell around the ammonium group. Tyr is the only amino acid considered here that is found to provide a competitive hydration site on the side chain. Structures **I** (four) and **J** (five H_2O molecules) are nearly isoenergetic (within 0.7 kcal/mol) with the respective B3LYP global minima **G** and **H**.

Dissusion

With the ammonium group formally carrying the ionic charge in $PheH^+$, $TrpH^+$, and $TyrH^+$, it is not surprising that this group competes successfully for water molecules due to the significant charge−dipole interaction bonus in addition to the hydrogen bond offered to water. The resulting theoretical binding energy of ∼14 kcal/mol agrees well with experiment (Table 1). What is surprising, though, is that the formally neutral carboxyl group is an equally good hydration site, with structure **A** (Figure 4) winning by a nearly insignificant 1 kcal/mol or less (B3LYP/6-311++G**) over **B** (Table 2). Consequently, the two H_2O molecules of the most stable doubly hydrated structure (**D**) occupy the hydration sites of **A** and **B** simultaneously, with theoretical and experimental binding energies of 11−12 kcal/mol for the second water molecule (Table 1).

Why is the carboxyl group such a competitive hydration site? Let us consider the geometry of the fully dehydrated molecules

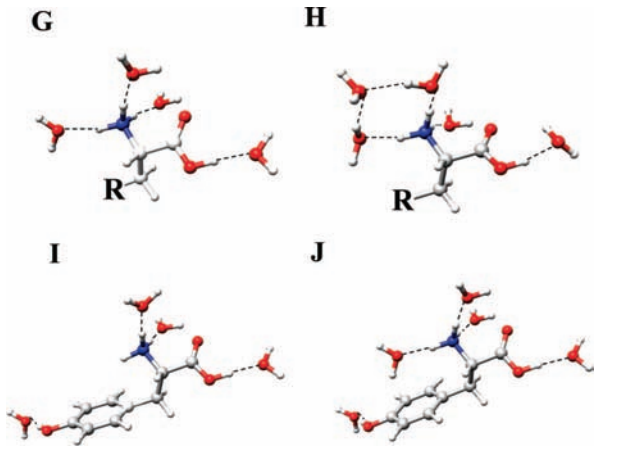

Figure 5. Hydration structures for protonated Phe, Trp, and Tyr with four (**G**) and five (**H**) H_2O molecules. The competitive structures with side chains hydrated are also shown for Tyr with four (**I**) and five (**J**) H_2O molecules. (R = C_6H_5, C_8NH_6, and C_6H_4OH for Phe, Trp, and Tyr, respectively.) Coordinates for all structures given in Supporting Information.

Table 2. Relative Energies[a] (in kcal/mol) for the Higher-Energy Hydrated Structures of Protonated Phe, Trp, and Tyr Shown in Figures 4 and 5

	H_2O B−A	$2H_2O$ C−D	$3H_2O$ E−F	$4H_2O$ I−G	$5H_2O$ J−H
Phe	1.0	0.7	1.7	N/A[b]	N/A[b]
Trp	0.5	1.7	1.6	N/A[b]	N/A[b]
Tyr	1.0	0.7	1.8	0.2	0.7

[a] Energies at 0 K for structures **B**, **C**, **E**, **I**, and **J** relative to the corresponding lowest-energy structures **A**, **D**, **F**, **G**, and **H**, respectively. [b] Not applicable. For Phe and Trp there are no structural analogues to **I** and **J**.

Scheme 1. Network of Interactions Involving the Ammonium Group in Protonated Amino Acids

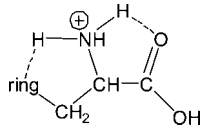

first. Very generally, the lowest energy structures of flexible polyatomic ions in the absence of solvent molecules are characterized by self-solvation of the charge.[14,35] As a result of charge solvation, two of the three protons of the charge-carrying ammonium group in the systems studied here are tied up in interactions[36] with both the carboxyl group and the side chain (Scheme 1), leaving only the third proton available for unobstructed interaction with a water molecule. Once this position is occupied, the second H_2O molecule may find alternatives to the ammonium group. An additional factor reducing the significance of the ammonium group as a hydration site is the fact that the ammonium group carries only 65% of the ionic charge according to a natural population analysis (NPA)[37] we carried out for $TrpH^+$. Nevertheless, intuitively we would expect that the highly ionic character of the ammonium group should still dominate hydration, especially for the first H_2O molecule.

(35) Wyttenbach, T.; vonHelden, G.; Bowers, M. T. *J. Am. Chem. Soc.* **1996**, *118*, 8355–8364.
(36) "Interactions" refers here to van der Waals interactions in the broadest sense, including (possibly weak) hydrogen bonds.
(37) Foster, J. P.; Weinhold, F. *J. Am. Chem. Soc.* **1980**, *102*, 7211–7218.

Table 3. Comparison of the Relative Energies of Two $ValH^+ \cdot 2H_2O$ Structures (in kcal/mol) Calculated at the MP2/6-311++G** and B3LYP/6-311++G** Levels[a]

	MP2/6-311++G**	B3LYP/6-311++G**
structure C[b]	0.0	1.2
structure D[c]	1.0	0.0

[a] Values corrected for BSSE and zero-point energy. [b] Both waters solvating the ammonium group. [c] One water solvating the ammonium group and one solvating the carboxyl group.

Scheme 2. Schematic Representation of the $-NH_3^+$ Orientation with Respect to the Carboxyl C=O Group for Singly and Doubly Hydrated Ammonium Groups (e.g., Structures **A** and **C**, Respectively)[a]

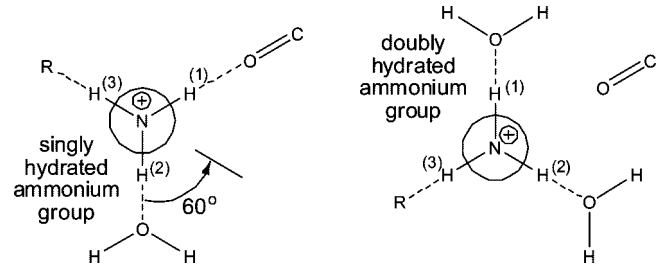

[a] A 60° counterclockwise rotation is indicated upon addition of the second water molecule. Orientation of the amino acid side chain R readjusts correspondingly. Note that the N, H(1), and O atoms involved in the ammonium−carboxyl interaction in structure **A** are not positioned on a straight line as they would in a typical hydrogen bond (Figure 4).

Previous B3LYP/6-31++G** calculations on $ValH^+$ yielded a similar result: structures **A** and **B** are close in energy, and the $ValH^+ \cdot (H_2O)_2$ structure **D** is slightly lower in energy than **C**.[25] However, whereas spectroscopic results presented in the same study agreed with theory for $ValH^+ \cdot H_2O$, the appearance of an unshifted COO−H stretch band in the spectrum of $ValH^+ \cdot (H_2O)_2$ (Figure 6 of ref 25) leads to the interpretation that both H_2O molecules sit on the ammonium group (structure **C**). Hence, the increased stability calculated for **D** over **C** may be an artifact of the theory used. To investigate this possibility further, we recalculated $ValH^+ \cdot (H_2O)_2$ at the level of theory employed in our present study (B3LYP/6-311++G**) and for comparison at the MP2/6-311++G** level (see Methods). We find that the $ValH^+$ B3LYP energies track the results of the aromatic amino acids faithfully, with structure **D** slightly lower in energy than **C** (Table 3). This result can now be compared to the MP2 calculations which confirm that structures **C** and **D** are very close in energy, with **C** slightly lower than **D** in this case. We conclude that structure **D** is indeed a low-energy structure, isoenergetic with **C** within 2 kcal/mol. We also conclude that the accuracy of our relative B3LYP/6-311++G** energies reported in Table 2 is of the order of ±1 kcal/mol.

For all amino acids Val, Phe, Trp, and Tyr, the conformations of the singly hydrated structures **A** and **B** and the doubly hydrated structure **D** are close to that of the fully dehydrated molecule. However, the conformation **C**, with hydrated ammonium hydrogen atoms H(1) and H(2), is somewhat, different with the ammonium group rotated around the $H_3N^+-C_\alpha$ bond by 60° (Scheme 2). Hence, neither of the ammonium H(1) and H(2) atoms interacts particularly strongly with the carbonyl O atom, since each of the H(1) and H(2) atoms forms a hydrogen bond with a water molecule instead, and the H(1)−carbonyl O distance is about equal to the H(2)−carbonyl O distance. The rotation of the ammonium group causes the side chain to change its orientation as well, leading to a conformation with an intact H(3)−side chain interaction.

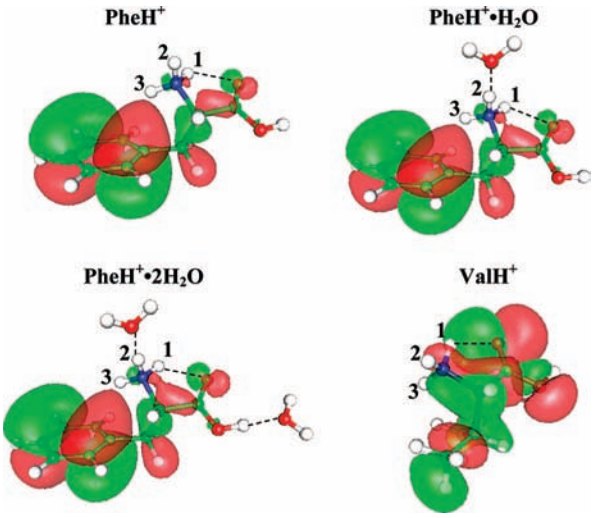

Figure 6. Plots of the highest occupied molecular orbital (HOMO) for $PheH^+$, $PheH^+ \cdot H_2O$, $PheH^+ \cdot 2H_2O$, and $ValH^+$.

Since the H(3)−side chain interaction is maintained in structures **A**−**D** upon addition of water molecules,[38] it is interesting to examine the type of interactions occurring in the amino acids studied here in some detail. Previous studies[39] show that hydrogen-bond-like interactions occur between an amide hydrogen atom and the cloud of aromatic π electrons in peptides. While several studies[39−43] indicate NH−π interactions are relatively weak (~2 kcal/mol for ammonia−benzene), they still are thought to play an important role in drug−protein binding[44] and in protein folding.[45] In contrast to most previous studies, here we are dealing with a charge-carrying ammonium group. However, the charge is not expected to inhibit formation of an NH−π hydrogen bond, and it may actually increase the interaction. Plots of the highest occupied molecular orbitals (HOMO) of the lowest-energy $PheH^+$, $PheH^+ \cdot H_2O$, and $PheH^+ \cdot (H_2O)_2$ structures (Figure 6) show that the delocalized π electrons spread over the benzene ring and extend, in fact, all the way to H(3) of NH_3^+, confirming the presence of an NH−π hydrogen bond. In contrast, the HOMO of $ValH^+$ (bottom right panel of Figure 6) does not show any interaction between the ammonium H(3) atom and the side chain involving an electron density distribution indicative of a chemical bond or hydrogen bond. Yet even though the ammonium−side chain interaction is very different and apparently more of a dipole−induced dipole and Lennard-Jones type in valine compared to the aromatic amino acids, a nearly identical NH_3^+ rotation and side chain adjustment (see Scheme 2) takes place in both valine and the aromatic amino acids during addition of a second water molecule to the ammonium group (structure **A** versus **C**). Hence, the exact nature of the NH−R interaction (H-bond vs induced dipole) affects neither the energetics nor the structural details involved in the transition from a singly to a doubly hydrated ammonium ion.

The H(1)−carboxyl interaction is present not only as a stabilizing structural element in the fully dehydrated amino acids but also in the doubly hydrated structure **D** and is likely at least partly responsible for the relative stability of structure **D** compared to **C**, where this interaction is absent. Another factor contributing to the stability of structure **D** is the intrinsically high hydrophilicity of the carboxyl group. The hydration energy we calculate for adding water to −COOH in neutral Trp is 7.8 kcal/mol, much higher than the amine−water binding energy of 4.6 kcal/mol. In the presence of a positive charge on the amine, the COOH−water interaction increases to 13.8 kcal/mol in $TrpH^+$, demonstrating the significant effect of the nearby charge. A glance at structures **B** and **D** in Figure 4 shows that the dipole of the carboxyl-bound water molecule lines up favorably with the positive charge on the ammonium group, explaining the increased water binding energy.

For systems containing two or more water molecules, the location and orientation of the various water dipole moments with respect to each other also contribute to the magnitude of the overall interaction energy. Here we evaluate the energetic contribution of the solvent−solvent interaction to the total energy in systems containing three water molecules. In structure **E** (Figure 4) the ammonium group is surrounded by three H_2O molecules, whereas in structure **F**, two H_2O molecules solvate $-NH_3^+$ and one −COOH. The solvent−solvent interaction energy is

$$\Delta E_s = E[(H_2O)_n] - nE[H_2O]$$

where $E[(H_2O)_n]$ is the energy of the H_2O molecules in the same arrangement as in $MH^+ \cdot (H_2O)_n$ (M = Phe, Trp, and Tyr) and $E[(H_2O)]$ the energy of an individual H_2O molecule. For structure **E** with a triply hydrated ammonium group (Figure 4), ΔE_s takes on a positive value of 3.3 kcal/mol for all three amino acids Phe, Trp, and Tyr (i.e., the net interaction is repulsive or unfavorable), whereas for structure **F** with a doubly hydrated ammonium group and a singly hydrated carboxyl group, ΔE_s is less positive, with a value of 1.7 kcal/mol. Hence, the water dipole interaction is less repulsive in **F** compared to **E**, thereby contributing to the increased stability of carboxyl hydrated structures like **F** over ammonium-only hydrated structures such as **E**.

Structures for increasingly hydrated systems are shown in Figure 5, and the corresponding water binding energies given in Table 1. The theoretical energies agree well with the experimental values, giving confidence in the theoretical structures. The optimized structures for protonated Phe and Trp with five H_2O molecules, structure **H**, indicate that the first solvation shell is completed as four H_2O molecules solvate the ammonium and carboxyl groups, and the fifth H_2O molecule binds to two water molecules, not directly to the amino acid.[46,47] The trend of $-\Delta S_n$ in Figure 3 (bottom panel) shows a substantial drop in magnitude from $-\Delta S_4$ to $-\Delta S_5$ and supports this result. Such a drop in solvation entropy has previously been

(38) At the B3LYP level of theory, the H(3)−side chain interaction is 2 kcal/mol stronger than the H(2)−carboxyl interaction, based on a comparison of structures having one or the other type of interaction. This result indicates that the H(3)−side chain interaction is significant and of the same order as the H(2)−carboxyl interaction or stronger.

(39) Rodham, D. A.; Suzuki, S.; Suenram, R. D.; Lovas, F. J.; Dasgupta, S.; Goddard, W. A.; Blake, G. A. *Nature* **1993**, *362*, 735–737.
(40) Zwier, T. S. *Annu. Rev. Phys. Chem.* **1996**, *47*, 205–241.
(41) Tsuzuki, S.; Honda, K.; Uchimaru, T.; Mikami, M.; Tanabe, K. *J. Am. Chem. Soc.* **2000**, *122*, 11450–11458.
(42) Mons, M.; Dimicoli, I.; Tardivel, B.; Piuzzi, F.; Brenner, V.; Millie, P. *Phys. Chem. Chem. Phys.* **2002**, *4*, 571–576.
(43) Vaupel, S.; Brutschy, B.; Tarakeshwar, P.; Kim, K. S. *J. Am. Chem. Soc.* **2006**, *128*, 5416–5426.
(44) Perutz, M. F.; Fermi, G.; Abraham, D. J.; Poyart, C.; Bursaux, E. *J. Am. Chem. Soc.* **1986**, *108*, 1064–1078.
(45) Chakrabarti, P.; Bhattacharyya, R. *Prog. Biophys. Mol. Biol.* **2007**, *95*, 83–137.

(46) A structure with three water molecules in the first solvation shell (like structure **F**) and one water in the second shell is detected, but found to be energetically less favorable than structure **G** (by 2−3 kcal/mol).

observed for a number of systems, and the effect is a clear signature of the start of a new solvation shell.[48,49]

For Tyr, considered a hydrophilic residue, the side-chain hydroxyl group (−OH) is found to be a competitive hydration site (structures **I** and **J** in Figure 5). Whereas the side-chain-hydrated $TyrH^+\cdot(H_2O)_n$ structure, $n = 2$, is calculated to be 3.5 kcal/mol less stable than structure **D**, the $n = 4$ and 5 structures **I** and **J** are approximately isoenergetic with structures **G** and **H**, respectively (Table 2). In contrast to the hydrophobic amino acids Phe and Trp, experimental hydration entropy values for Tyr (Figure 3) do not provide evidence for the start of a new solvation shell for the fifth water molecule, with values of −20.9 and −20.5 cal/(mol·K) for ΔS_4 and ΔS_5, respectively, supporting the significance of structure **J**.

Conclusions

1. In protonated aromatic amino acids, the charge-carrying ammonium group offers only one fully exposed hydration site able to host a water molecule, with a binding energy of 13 kcal/mol.

2. The neutral carboxyl group provides a second fully exposed hydration site that competes successfully for water, with a binding energy comparable to that of the ammonium group.

3. Additional water binding sites include the two less exposed sites on the ammonium group and the side-chain hydroxyl group in tyrosine, with water binding energies between 8 and 11 kcal/mol.

4. Water bound in a second solvation shell around the ammonium group is bound by 7−8 kcal/mol.

5. Reasons for the high water affinity of the carboxyl group are an intrinsically high hydrophilicity, favorable charge−dipole alignment, favorable dipole−dipole interaction among water molecules in multiply hydrated species, and the lack of alternative fully exposed hydration sites.

Acknowledgment. Dr. Catherine J. Carpenter's significant contribution in the editing process of this paper is highly appreciated. The support of the National Science Foundation under grant CHE-0503728 is gratefully acknowledged.

Supporting Information Available: Complete refs 31 and 32; atomic coordinates and absolute energies of all structures presented in the figures. This material is available free of charge via the Internet at http://pubs.acs.org.

JA8085017

(47) Structure **H**, corresponding to structure **G** with an additional fifth water molecule bound to water attached to H(2) and H(3), is the lowest-energy structure located for a five-water complex. However, additional structures in the same family (**G** plus one water in the second solvation shell) include structures with a fifth water molecule bound between H(3) and H(1) and between H(1) and H(2) with similar energies (isoenergetic within 1−2 kcal/mol).

(48) Kemper, P. R.; Weis, P.; Bowers, M. T.; Maitre, P. *J. Am. Chem. Soc.* **1998**, *120*, 13494–13502.

(49) Manard, M. J.; Kemper, P. R.; Bowers, M. T. *Int. J. Mass Spectrom.* **2005**, *241*, 109–117.